CALCULATION SCHEME OF REINFORCED CONCRETE STRUCTURES OF CIRCULAR CROSS-SECTION UNDER BENDING WITH TORSION

Vladimir I. Kolchunov [1], *Sergey A. Bulkin* [2]

[1] South-West State University, Kursk, RUSSIA,
[2] Urban planning institute of residential and public buildings (GORPROJECT), Moscow, RUSSIA

Abstract. The developed design diagram of the ultimate resistance of reinforced concrete structures in bending with torsion of circular cross-sections most fully reflects the features of their actual exploitation. For a spatial crack of a diagonal large ellipse, sections are taken in the form of a swirling propeller with concave and convex spatial parabolas from the first and second blocks between vertical transverse circular sections from the beginning to the end of the crack. For practical calculations in compressed and tensioned concrete, a polyline section of three sections is considered: two longitudinal trapezoids and the third middle section of the radius curve of a small ellipse close to forty-five degrees. When calculating unknown forces, solutions of the equations of equilibrium and deformations of the sections are made up to the end of the crack passing through the moment points for the resultant moments and the projections of internal and external forces. Shear torsional stresses along the linear longitudinal sections of the trapezoid were presented, as well as normal and shear stresses located on the end cross-sections at a distance x from the support. The height of the compressed area of concrete decreases with an increase in bending moments in the spatial section between the first and third cross-sections. It is found in their relationships and connections. The dowel action of reinforcement is determined using a special model of the second level with discrete constants. The static loading scheme was considered from the standpoint of an additional proportional relationship between the torques along the length of the bar in the spatial section and the first and third transverse sections. For a dangerous spatial crack, when projected onto the horizontal axis, the length C was found from a diagonal large ellipse of a round bar.

Keywords: reinforced concrete, circular section, calculation scheme, bending moment, torsion, spatial crack, dangerous spatial crack, governing equations

РАСЧЕТНАЯ СХЕМА КРУГЛЫХ ЖЕЛЕЗОБЕТОННЫХ КОНСТРУКЦИЙ ПРИ СЛОЖНОМ ПРЕДЕЛЬНОМ СОПРОТИВЛЕНИИ-КРУЧЕНИИ С ИЗГИБОМ

Вл.И. Колчунов [1], *С.А. Булкин* [2]

[1] Юго-Западный государственный университет, г. Курск, РОССИЯ
[2] ЗАО «Городской проектный институт жилых и общественных зданий», г. Москва, РОССИЯ

Аннотация. Разработанная расчетная схема предельного сопротивления железобетонных конструкций при кручении с изгибом элементов с круглыми поперечными сечениями наиболее полно отражает особенности их действительной работы. Для пространственной трещины диагонального большого эллипса приняты сечения в виде закрученного пропеллера с вогнутой и выпуклой пространственными параболами из первого и второго блоков между вертикальными поперечными круглыми сечениями от начала до конца трещины. Для практических расчетов в сжатом и растянутом бетоне рассмотрено ломанное сечение из трех участков, – два продольных трапеции и третий средний близкий к сорока пяти градусам участок кривой радиуса малого эллипса. При расчете неизвестных усилий составлены разрешающие уравнения равновесия и деформаций поперечных сечений до конца трещины, проходящие через моментные точки для равнодействующих моментов и проекций внутренних и внешних сил. Были представлены касательные напряжения кручения по линейным продольным сечениям трапеции, а также нормальные и касательные напряжения, расположенные на концевых поперечных сечениях на расстоянии x от опоры. При этом с увеличением изгибающих моментов уменьшаются высоты сжатой области бетона в простран-

ственном сечении между первым и третьим поперечными сечениями, которые могут быть найдены из их отношений и связей. Учитывается «нагельный» эффект в растянутой продольной и поперечной арматуре, определяемый с привлечением специальной модели второго уровня с дискретными константами. Статическая схема нагружения рассматривалась с позиций дополнительного пропорционального соотношения между крутящими моментами по длине стержня в пространственном сечении и в поперечных первом и третьем сечениях. При этом для опасной пространственной трещины при проецировании на горизонтальную ось была найдена длина C из диагонального большого эллипса круглого стержня.

Ключевые слова: железобетонные конструкции, круглое сечение, расчетная схема, прочность, изгибающий момент, крутящий момент, опасная пространственная трещина, разрешающие уравнения

INTRODUCTION

In regard with the complication of the types of actions on building structures, the creation of calculated models and the construction of calculated diagrams of the complex resistance of reinforced concrete in torsion with bending becomes more and more urgent [1, 2, 3]. This is also due to the fact that, firstly, there are relatively few such studies [3–9], and secondly, with the noted actions, it is necessary to take into account the spatial work of the overwhelming majority of reinforced concrete structures with more and more original architectural and structural solutions of buildings and structures. The existing modern calculated models of reinforced concrete, the analysis of which is given, for example [6], does not fully take into account the features of the resistance of complexly stressed reinforced concrete elements after cracking, including the very scheme of cracks, taken in the calculation with different cross-section sizes and not always confirmed experimentally.

Therefore, the purpose of this research is to develop a calculated diagram of the ultimate resistance of reinforced concrete structures in torsion with bending for circular cross-sections, which most fully reflects the features of their resistance after cracking [2, 12, 17, 18].

METHODS

To determine the calculated forces, the resolving equations of equilibrium and deformations are drawn up. In this case, the projection of a dangerous spatial crack is determined through the diagonal (larger) ellipse of the round bar [13].

As a result, for a reinforced concrete structure of a beam in a circular cross-section, we obtain a spatial crack and, accordingly, a calculated scheme after its formation. In this case, there are cross-sections from sections 1-1 at the beginning to 3-3 at the end of the spatial crack - an ellipse for the first and second blocks (Figure 1). We obtain a calculated diagram of the resistance of a reinforced concrete beam of a circular cross-section from the action of combined bending with torsion, taking into account a spatial crack. In compressed concrete, there are three zones l_1, l_2, l_3, - longitudinal zones (and), as well as an ellipse in the zone l_2 (Figure 2). In tensioned concrete, the same three zones l_1, l_2, l_3, are located, but the ellipse is adopted for the zone l_2, as well as a parabola for the zones l_1 and l_3.

The equation of a small ellipse for a spatial section is:

$$\frac{y^2}{2R^2} + \frac{z^2}{R^2} = 1 . \tag{1}$$

Here $b = R$; $a = \dfrac{R}{\cos\alpha} = \dfrac{R}{\cos 45°} = R\sqrt{2}$.

Then, in stretched concrete in the first and second sections, we have spatial curves of the form $f_{par1,2,3}(x, y, z)$.

To construct the first spatial parabola

$f_{par1,2,3}(x,y,z)$, we find the coordinate T.1 (x, y, z) along the x-axis ($x = -l_1 - 0.5l_2$) belonging to the circle in section 1-1 in a plane parallel to the Ozy plane. Then, for the coordinate at the desired point, we can write:
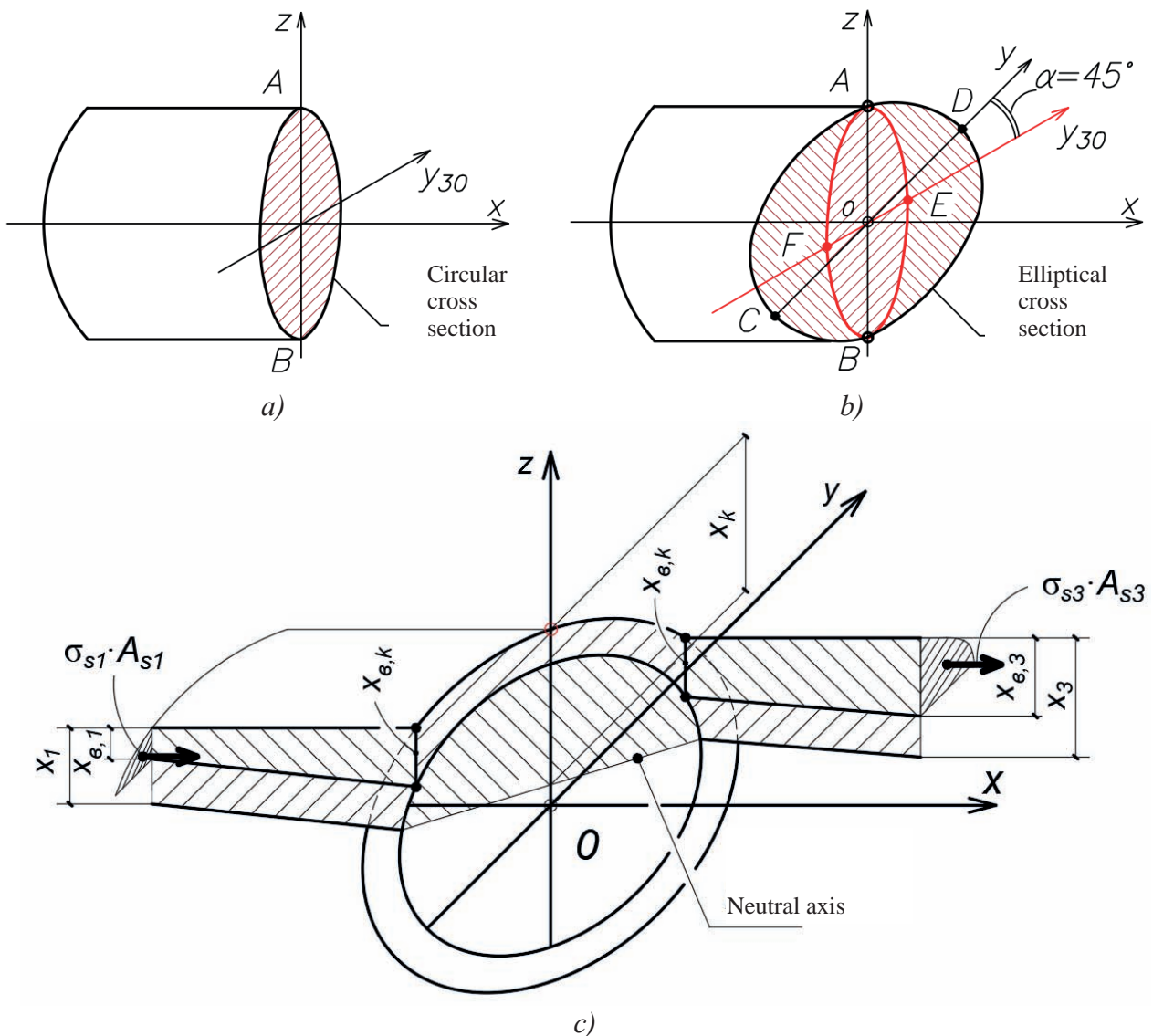
$$y = \pm\sqrt{R^2 - (R - x_k)^2} . \qquad (2)$$

Now we find the ordinate of T.2 (x, y, z) along the x-axis ($x = -0.5l_2$) belonging to a small ellipse lying in the plane Ozy ($z = -R + x_k - \Delta x_1 - x_{b,k}$):

$$y = \pm\sqrt{R^2 - (-R + x_k - \Delta x_1 - x_{b,k})^2} . \qquad (3)$$

For a point lying in the plane of the coordinate axes Oyz we have the following coordinate values: x = 0; y = 0; z = -R.

Figure 1. *To the construction of an elliptical calculated scheme of a spatial crack in a reinforced concrete structure with a circular cross-section: a) a circular cross-section; b) elliptical section; c) the layout of the broken cross-section for compressed concrete*

a)

Cross section 1-1

Cross section 3-3

b)   *c)*
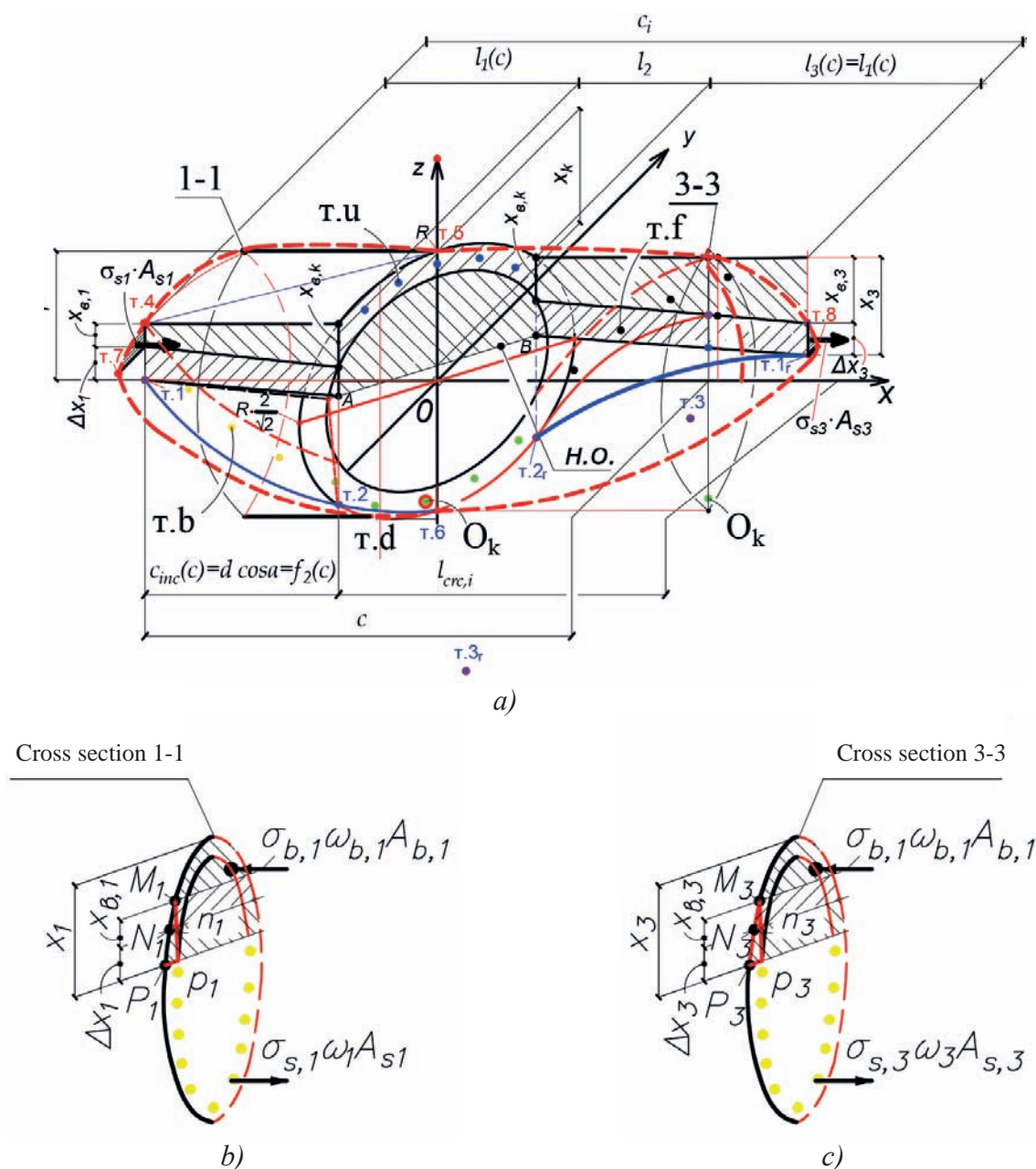
Figure 2. Calculated scheme for determining the ultimate resistance of a reinforced concrete structure in a complex stress state - torsion with bending: a spatial crack for a large ellipse with a swirling propeller in the direction of concave and convex spatial parabolas coming from the first and second blocks (a) and located between circular cross-sections I – I (b) and 3-3 (c)

Let's define the coefficients A_1, B_1, C_1 for the auxiliary curve $z_1(x) = A_1 \cdot x^2 + B_1 x + C_1$. To do this, we substitute the values of the coordinates at points 1, 2, 3 into the equation of this curve. After algebraic transformations, we get:

$$A_1 = \frac{2R - x_1 - x_k + \Delta x_1 + x_{b,k}}{(l_1 + 0.5l_2)^2 - (-0.5l_2)^2}; B_1 = 0; \quad (4)$$

$$C_1 = R - x_1 - \frac{2R - x_1 - x_k + \Delta x_1 + x_{b,k}}{(l_1 + 0.5l_2)^2 - (-0.5l_2)^2}(l_1 + 0.5l_2)^2 . (5)$$

Similarly, the values of the coefficients A_2, B_2, C_2 of the auxiliary plane curve are obtained, we obtain:

$$A_2 = \frac{\sqrt{R^2 - (R - x_1)^2} - \sqrt{R^2 - (-R + x_k - \Delta x_1 - x_{b,k})^2} - \dfrac{\sqrt{R^2 - (R - x_1)^2}}{(l_1 + 0.5l_2)} l_1}{(-0.5l_2)^2 - (-l_1 - 0.5l_2)^2} ; \qquad (6)$$

$$B_2 = \frac{\sqrt{R^2 - (R - x_1)^2}}{(l_1 + 0.5l_2)} ; \qquad (7)$$

$$C_2 = -\frac{\sqrt{R^2 - (R - x_1)^2} - \sqrt{R^2 - (-R + x_k - \Delta x_1 - x_{b,k})^2} - \dfrac{\sqrt{R^2 - (R - x_1)^2}}{(l_1 + 0.5l_2)} l_1}{\left((-0.5l_2)^2 - (-l_1 - 0.5l_2)^2\right) \cdot (l_1 + 0.5l_2)^2} . \qquad (8)$$

Let us write the equation of the first spatial parabola $f_{par1,2,3}(x, y, z)$:

$$f_{par1,2,3}(x, y, z) = \sqrt{z_1(x)^2 + y_1(x)^2}. \qquad (9)$$

To construct the second spatial parabola $f_{par1_r,2_r,3_r}(x, y, z)$ we define the coordinates of points 1r, 2r, and 3r (see Figure 2), which have coordinates similar to points 1,2 and 3:

$$m.1_r(0.5l_2 + l_3; \sqrt{R^2 - (R - x_3)^2}; R - x_3); \qquad (10)$$

$$m.2_r(0.5l_2; \sqrt{R^2 - (-R + x_k - \Delta x_3 - x_{b,k})^2}; -R + x_k - \Delta x_3 - x_{b,k}); \qquad (11)$$

$$m.3_r(0.5l_2 - l_3; \sqrt{R^2 - (-R + x_3)^2}; -R + x_3). \qquad (12)$$

Then we can calculate the coefficients A_3, B_3, C_3 for the auxiliary curve $z_2(x) = A_3 \cdot x^2 + B_3 x + C_3$. To do this, substitute the values of coordinates at points 1r, 2r, 3r into the equation of this curve, and after algebraic transformations we obtain:

$$A_3 = \frac{(2R - x_3 - x_k + \Delta x_3 + x_{b,k})2l_3}{(2l_3 + 0.5l_2)(0.5l_2 + l_3)^2 + (0.5l_2 + l_3)^3 - (0.5l_2 - l_3)^2(l_3) - (0.5l_2)^2 \cdot 2l_3} ; \qquad (13)$$

$$B_3 = \frac{-A_3 \cdot (0.5l_2 + l_3)^2 + A_3 \cdot (0.5l_2 - l_3)^2}{2l_3} ; \qquad (14)$$

$$C_3 = \left(-R + x_k - \Delta x_3 - x_{b,k}\right) - A_3 \cdot \left(\frac{(0.5l_2)^2 \cdot 2l_3 - (0.5l_2 + l_3)^2(0.5l_2) + (0.5l_2 - l_3)^2(0.5l_2)}{2l_3}\right). \qquad (15)$$

The coefficients A_4, B_4, C_4 for the auxiliary plane curve $y_2(x)$ are obtained in a similar way:

$$A_4 = \frac{B_4(2l_3)}{(0.5l_2 - l_3)^2 - (0.5l_2 + l_3)^2} ; \qquad (16)$$

$$B_4 = \frac{\left((0.5l_2 - l_3)^2 - (0.5l_2 + l_3)^2\right) \cdot \left(\sqrt{R^2 - (R - x_3)^2} - \sqrt{R^2 - (-R + x_k - \Delta x_3 - x_{b,k})^2}\right)}{(2l_3 - 1) \cdot (0.5l_2 + l_3)^2 - (2l_3) \cdot (0.5l_2)^2 + l_3 \cdot (0.5l_2 - l_3)^2} ; \qquad (17)$$

$$C_4 = \sqrt{R^2 - (-R + x_k - \Delta x_3 - x_{b,k})^2} - \frac{B_4 \cdot \left((2l_3) \cdot (0.5l_2)^2 + (0.5l_2)(0.5l_2 - l_3)^2 - (0.5l_2)(0.5l_2 + l_3)^2\right)}{(0.5l_2 - l_3)^2 - (0.5l_2 + l_3)^2}. \quad (18)$$

By analogy with Eq. (9), the equation of the second spatial parabola is also written:

$$f_{par1_r,2_r,3_r}(x, y, z) = \sqrt{z_2(x)^2 + y_2(x)^2}. \quad (19)$$

From the equilibrium equation of the moments of internal and external forces in section I – I relative to the y-axis passing through the point of application of the resultant forces O_I in the stretched reinforcement ($\sum M_{O,I} = 0$), we obtain:

$$M_{bend,I} = R_{\sup,I,M} \cdot a_{m,I} = \varphi_{10,*} \cdot \sigma_{bu,x,I} A_{b,I} [h_0 - \varphi_{z,cir} \cdot x] +$$
$$+ m \cdot R_{sc,I,up} \cdot \omega_{up,cir} \cdot A_{sc,up} (h_0 - a'_s) +$$
$$+ \sum R_{sc,I,i,lef} \cdot \omega_{c,cir} \cdot A_{sc,I,i,lef} (h_0 - a'_{s,i,lef}) +$$
$$+ \sum R_{sc,I,i,rig} \cdot \omega_{c,cir} \cdot A_{sc,I,i,rig} (h_0 - a'_{s,i,rig}) -$$
$$- \sum R_{s,I,i,lef} \cdot \omega_{cir} \cdot A_{s,I,i,lef} (a_{s,i,lef} - a_{s,d}) -$$
$$- \sum R_{s,I,i,rig} \cdot \omega_{cir} \cdot A_{s,I,i,rig} (a_{s,i,rig} - a_{s,d}) -$$
$$- K_M K_{pr,M} \cdot R_{\sup,I} - R_{\sup,I} \cdot a = 0. \quad (20)$$

Here $\varphi_{10,*}$ is the parameter that takes into account the procedure for projecting the stress components in the k plane onto the I – I plane perpendicular to the longitudinal axis of the reinforced concrete element; sign * - means the reverse transition from section k, in the upper fiber of which the deformation criterion of strength is "triggered," to section I – I through the transition relations of projection of the diagram $\sigma_i - \varepsilon_i$ to the direction perpendicular to the plane k (see Figure 2); product $\varphi_{10,*}\sigma_{bu,x,I}A_b$ - the value for the considered section is known; $\sigma_{b,u} = \text{const}$; $A_b = R^2 \arccos((R - x_1)/R) - (R - x_1)\sqrt{2Rx_1 - x_1^2}$ - area of the compressed concrete zone in section 1-1; x_1 - the height of the compressed concrete zone in section 1-1; $h_0 - \varphi_{z,cir} \cdot x$ - shoulder of the inner pair to the

center of the compressed zone of concrete; $\varphi_{z,*}$ - a static-geometric parameter that takes into account the location of the center of gravity of the compressed zone of concrete in section I – I (in the section x_B, the height of the compressive stress diagram is taken in the form of a pipe sector, in the section $x - x_B$ - in the form of an ellipse sector); K_M - a numerical coefficient that takes into account the static loading scheme from the standpoint of additional bending moments along the length of the bar. It is used when it is necessary to take into account the field of local stresses Δ_M and is found according to the proposals of S.P. Tymoshenko. Thus, it can be considered Δ_M a known quantity; $K_{pr,M}$ - coefficient, ratio (it is known and specified in the initial data is given) by the generalized support reaction $R_{\sup}$ and bending moment M; $R_{\sup}$ - generalized support reaction in the first block at the moment of exhaustion of the bearing capacity of the reinforced concrete structure of the beam; a - horizontal distance from the support of the beam to the section I – I; $\omega_{up,cir}$ - the filling factor of the diagram for the upper compressed reinforcement; ω_{cir} - coefficient of filling the diagram of a stretched right or left reinforcement; $\omega_{c,cir}$ - coefficient of filling the diagram of compressed right or left reinforcement.

The unknown $M_{bend,I}$ is found from this equation (20).

Next, we obtain an expression for the transverse force from internal forces:

$$Q_I = R_{\sup,I,M} = \frac{M_{bend,I}}{a_{m,I}}. \quad (21)$$

Here $M_{bend,I}$ is found from equation (20)

$$a_{m,I} = a + \mathrm{K}_\mathrm{M} K_{pr,M} ; \qquad (22)$$

From the equilibrium equation of the projections of all forces acting in section I – I on the x-axis, the area of the compressed concrete zone $A_{b,I}$ in this section is determined ($\sum X = 0$):

$$A_{b,I} = R^2 \arccos\left((R - x_1)/R\right) - (R - x_1)\sqrt{2Rx_1 - x_1^2} =$$
$$= \frac{1}{\varphi_{10,*}\sigma_{bu,x,I} \cdot \varphi_{y,*}} \cdot \Big[m \cdot R_{s,I,d} \cdot \omega_{d,cir} \cdot A_{s,d} -$$
$$- m \cdot R_{sc,I,up} \cdot \omega_{up,cir} \cdot A_{sc,up} - \sum R_{sc,I,lef} \cdot \omega_{c,cir} \cdot A_{sc,I,lef} -$$
$$- \sum R_{sc,I,rig} \cdot \omega_{c,cir} \cdot A_{sc,I,rig} + \sum R_{s,I,lef} \cdot \omega_{cir} \cdot A_{s,I,lef} +$$
$$+ \sum R_{s,I,rig} \cdot \omega_{cir} \cdot A_{s,I,rig} \Big]. \qquad (23)$$

From here, knowing the radius of the circle, you can calculate the height of the compressed zone of concrete x_1 in this section.

In equation (23) $\omega_{d,*}$ - the filling factor of the tensile reinforcement diagram; ω – the same, tensioned reinforcement right or left, ω_{up} – the same, compressed reinforcement, ω_{up} – the same, compressed reinforcement right or left; $R_{s,I,d}$, $R_{s,I,rig}$, $R_{s,I,lef}$ $R_{sc,I,up}$, $R_{sc,I,rig}$, $R_{sc,I,lef}$, R_{sw} - respectively, calculated resistances of tensile reinforcement, tensile reinforcement of right or left, compressed reinforcement, compressed reinforcement of right or left, clamps.

Similarly, from the equilibrium equation of the projections of all forces acting in section III – III on the x axis, the area of the compressed concrete zone $A_{b,3}$ in this section is determined ($\sum X = 0$):

$$A_{b,3} = R^2 \arccos\left((R - x_3)/R\right) - (R - x_3)\sqrt{2Rx_3 - x_3^2} =$$
$$= \frac{1}{\varphi_{10,*}\sigma_{bu,x,3} \cdot \varphi_{y,*}} \cdot \Big[m \cdot R_{s,3,d} \cdot \omega_{d,*} \cdot A_{s,d} -$$
$$- m \cdot R_{sc,3,up} \cdot \omega_{up} \cdot A_{sc,up} - \sum R_{sc,3,lef} \cdot \omega_c \cdot A_{sc,3,lef} -$$
$$- \sum R_{sc,3,rig} \cdot \omega_c \cdot A_{sc,3,rig} + \sum R_{s,3,lef} \cdot \omega \cdot A_{s,3,lef} +$$
$$+ \sum R_{s,3,rig} \cdot \omega \cdot A_{s,3,rig} \Big]. \qquad (24)$$

From here, knowing the radius of the circle, you can calculate the height of the compressed zone of concrete x_3 in this section.

Now we obtain an expression for the torque from internal forces in section I-I (see Figure 3) from the equation of the sum of the torques relative to the point b₁ ($\sum T_{b,I} = 0$):

$$M_{t,I} = \tau_{pl,u} \cdot \lambda x_1 \cdot b_{cir} \cdot \varphi_{cir,\tau} \cdot \left(z_1 - 0.5 \cdot \lambda x_1\right) +$$
$$+ 0.5 \cdot \tau_{pl,u} \cdot \left(x_1 - \lambda x_1\right) \cdot b_{cir} \cdot \left[0.5 \cdot \lambda x_1 + \frac{1}{3} \cdot \left(x_1 - \lambda x_1\right)\right] +$$
$$+ Q_s A_s \cdot \left(h_0 - z_1\right) \qquad (25)$$

Here $\varphi_{cir,\tau}$ is a parameter that takes into account the position of the center of gravity of the section; b_{cir} - the width of a segment of a circle in the section under consideration; $z_1 = R - \dfrac{S}{A}$ - distance from point b₁ to the center of gravity of the section; S - the static moment of the section; A - area of a circle; λx_1 - the height of the plastic deformation zone, $b_{cir} = 2\sqrt{R^2 - (R - x_k)^2}$.

From the equilibrium equation of the projections of internal and external forces acting in section I – I on the Y axis ($\sum Y = 0$), it is possible to determine the parameter $k_{Q,m}$ that takes into account the presence of adjacent cracks:

$$-\tau_{pl,x} \cdot x \cdot b - \tau_{pl,x} \cdot k_{Q,m} \cdot \left(h_0 - x\right) \cdot b + \mathrm{K}_\mathrm{M} \cdot R_{sup} = 0, \quad (26)$$

Here K_M – the same as in the formula (20).

In formula (26), the thrust forces in the working reinforcement in the middle section I – I are taken equal to zero.

In this case, the transverse force perceived by the concrete in the compressed zone will be equal to:

$$Q_{I,b} = \tau_{pl,x} \cdot x \cdot b . \qquad (27)$$
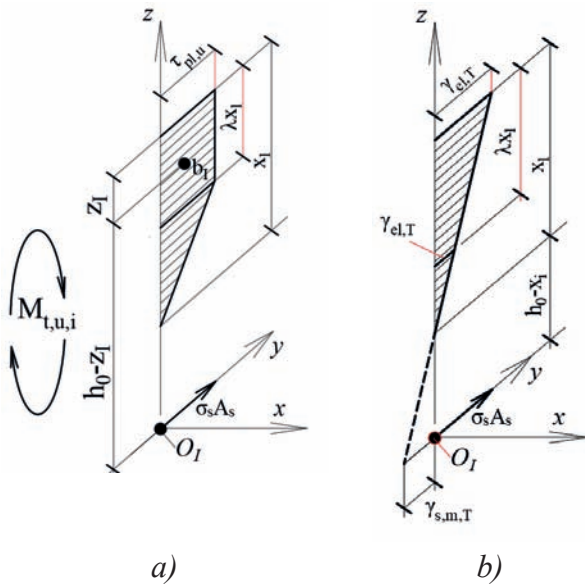
a)   *b)*

Figure 3. Diagrams of forces in cross-section I-I (3-3) with torsion

In turn, the shear force perceived by the concrete in the tensile zone will be (Figure 4):

$$Q_{II,T} = \tau_{pl,x} \cdot k_{Q,m} (h_0 - x) \cdot b. \qquad (28)$$

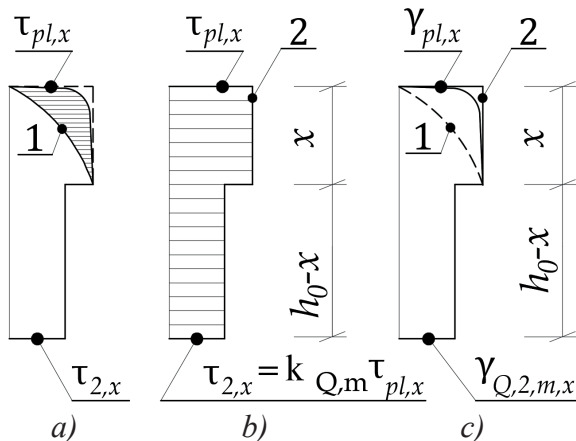On the other side:

$$Q_{II,T} = Q - Q_{I,b}. \qquad (29)$$

a)   *b)*   *c)*

Figure 4. Diagram of shear stresses τ_Q in the middle cross-sections $I - I$ (3-3)

Equality (26) can be used to determine the parameter $k_{Q,m}$ that takes into account the presence of adjacent spatial cracks in the stress-

strain state of the stretched zone of the middle cross-section I – I:

$$k_{Q,m} = \frac{K_M \cdot R_{sup} - \tau_{pl,x} \cdot x \cdot b}{\tau_{pl,x}(h_0 - x) \cdot b}. \qquad (30)$$

The formulation of the following equations requires some clarification. The upper, lower and lateral longitudinal reinforcement (in the presence of multi-tiered reinforcement) was conventionally not shown in Figure 2. Under equilibrium conditions, the stresses arising in the noted reinforcement are taken into account. The only exception is the equation of equilibrium of the moments of internal and external forces acting in section I – I relative to the axis x perpendicular to this section and passing through point b_k - the point of application of the resultant forces in the compressed zone ($T_{b, I} = 0$)

In the spatial section *k* for block 2, cut off by a complex section, passing along a spiral-shaped spatial crack and along a broken section of the compressed zone, all reinforcement [12] falling into this section is taken into account (see Figure 2). In this case, in the compressed upper longitudinal reinforcement, cut off by sections I – I and III – III (the dagger effect is not taken into account), and in the rest of the longitudinal and transverse reinforcement, the components of the dagger effect are taken into account. These components are determined using a special second-level model [1, 2, 13, 15].

The need to use a complex broken section of the compressed zone of concrete is due to the fact that its destruction occurs (as shown by experimental studies) in a certain volume located not along the entire length between points A and B (see Figure 2), but only in a certain volume located in the middle part of this volume. In this case, destruction occurs in the middle part not along the line AB, but at an angle close to 45° to the upper surface of the reinforced concrete structure, which predetermined the direction of the middle part

of the broken section, where the ultimate stress-strain state is reached.

In the areas of the compressed zone located at the edges of the broken section, the stress-strain state changes from sections I – I and III – III to the middle zone according to linear dependences, respectively. In this case, the height of the compressed zone decreases with an increase in the bending moment (see Figure 2). Such a design scheme is most consistent with the actual resistance of structures in torsion with bending, the parameters of which are experimentally confirmed.

The lateral surfaces of the broken section in compressed concrete coincide with the planes of the axis (or "smeared" plane) of the longitudinal working reinforcement. In this case, the reinforcement located in the lateral zones of the section when crossing the broken section is considered to be located on the left for section I – I and on the right for section III – III. Thus, it is intersected by planes I – I, III – III, respectively, at the end sections of a complex broken section.

The equations for determining the shear stresses from torsion in a cross-section located at a distance x from the support are written in cylindrical and Cartesian coordinates.

It is also important to note that all geometric characteristics are considered relative to the geometric center of the section.

With regard to the average cross-section I – I, which is in conditions of complex resistance - torsion with bending, it is advisable to take into account the fact that a significant part of this section is subject to tension. It is known [1, 2, 15] that in tensile concrete there are a number of adjacent spatial cracks that affect the stress-strain state of the middle section I – I. We will take into account this effect of adjacent cracks using the parameter $k_{T,m}$.

If the torque along the longitudinal axis of the reinforced concrete structure is not constant, but changes, then an additional dependence is introduced into the calculation, the ratio between the torques in section k and in section I – I:

$$\frac{K_T \cdot K_{pr,T} \cdot M_{T,I}}{M_{T,k}} = \frac{a}{c - 0,5b \cdot \sin \alpha},$$

$$M_{T,I} = \frac{a \cdot M_{T,k}}{K_T \cdot K_{pr,T} \cdot (c - 0,5b \cdot \sin \alpha)}. \quad (31)$$

Here K_T is a numerical coefficient that takes into account the static loading scheme from the standpoint of additional torques along the length of the bar; $K_{pr,T}$ - coefficient taking into account the ratio between R_{sup} and T; a is the horizontal distance from the structural support to the section I – I.

If the torque along the longitudinal axis of the reinforced concrete structure has a constant value, then the resulting stresses from torsion in stage III reach their limiting values equal to τ_u.

Knowing τ_u, we can determine the torque per j-th square of the compressed zone in section I – I by the formula:

$$T_c = M_{t,c} = \frac{\tau_{t,u} \cdot I_t}{\sqrt{(\zeta y)^2 + z^2}}. \quad (32)$$

In the case when the torque along the longitudinal axis of the reinforced concrete structure changes and has a lower value than in section k, then instead of τ_u, should be inserted τ_{sum} into formula (32).

In turn, the torque received by the concrete in the tension zone will be equal to:

$$T_R = M_{t,R} = \frac{\tau_{t,u} \cdot k_{T,m} \cdot I_t}{\sqrt{(\zeta y)^2 + z^2}}, \quad (33)$$

here $k_{T,m}$ is a parameter that takes into account the presence of adjacent spatial cracks in the stress-strain state caused by the torsion of the tensioned zone of the middle cross-section I – I. On the other hand, again returning to the construction of general resolving equations (see Figure 3), for $M_{t,R}$, the equation of equilibrium

of the moments of internal and external forces acting in section I-I relative to the x axis, perpendicular to this section and passing through the point of application can be used resultant forces b_I in the compressed zone of concrete ($T_{b,I} = 0$):

$$M_{t,R} = M_t - M_{t,c}. \qquad (34)$$

The parameter can be found from this equation $k_{T,m}$:

$$k_{T,m} = \frac{(M_t - M_{t,c})\sqrt{(\zeta y)^2 + z^2}}{\tau_{t,u} \cdot I_t}. \qquad (35)$$

Here $\tau_{t,u}$ is the shear torsional stress in compressed concrete, obtained in the third stage of stress-strain state by projecting the diagram "$\sigma_i - \varepsilon_i$" onto the section plane I – I for the dependence "$\tau - \gamma$", taking into account the ratio $Q{:}T$ or $M{:}T$, one of which, as a rule, is given. If necessary, one should take into account the additional dependence arising from the ratio of the torques in section 1–1 and in section k.

It is also appropriate to note that the limiting stresses $\tau_{t,u}$, $\tau_{t,xy,ul}$, $\tau_{t,zx,ul}$, $\sigma_{b,ul}$ are known (they are located on the horizontal sections of the "strain-stress" relationship diagrams), since the plastic state occurs simultaneously for tangential and normal stresses.

From the hypothesis of proportionality of longitudinal deformations in the calculated section, we find stresses in longitudinal reinforcement:

$$\sigma_{s,I} = \frac{\phi_{10,*}\sigma_{bu,x,I} \cdot E_s(\lambda)}{E_b(\lambda)} \cdot \frac{h_0 - x}{x} + \sigma_0 \leq R_{s,I}. \qquad (36)$$

Here σ_0 – prestresses in the stressed reinforcement at the moment when the prestress value in concrete decreases to zero when the structure is loaded by external forces, taking into account the prestress losses corresponding

to the considered stage of the structure operation. If the condition (36) is not met, then we assume $\sigma_{s,I}$ to be equal $R_{s,I}$. In equation (36), the notation $\phi_{10,*}$ is the same as in formula (20).

Normal shortening deformations along the x-axis in compressed concrete at various points of the k-k section and in the I-I section can be found from the same hypothesis of proportionality to the limiting deformations $\varepsilon_{bu,k,rig,x}$ at the rightmost point of the k-k section:–from the right point (rig) to the section I-I, –

$$\frac{\varepsilon_{b,I}}{\varepsilon_{bu,k,rig,x}} = \frac{a}{a - l_1}; \qquad (37)$$

$$\varepsilon_{b,I} = \frac{\varepsilon_{bu,k,rig,x} \cdot a}{a - l_1}. \qquad (38)$$

– rom the right point (rig) to the middle point (b_k):

$$\frac{\varepsilon_{bu,k,rig,x}}{\varepsilon_{b,k,x}} = \frac{a - l_1}{a - \left(l_1 + \frac{\sqrt{2}}{2}l_2 \cdot \frac{1}{2} - \eta_{hor,b} \cdot l_2\right)}; \qquad (39)$$

$$a_{m,b} = a - \left(l_1 + \frac{\sqrt{2}}{2}l_2 \cdot \frac{1}{2} - \eta_{hor,b} \cdot l_2\right); \qquad (40)$$

$$\varepsilon_{b,k,x} = \frac{\varepsilon_{bu,k,rig,x} \cdot a_{m,b}}{a - l_1} =$$
$$= \frac{\varepsilon_{bu,k,rig,x} \cdot \left[a - \left(l_1 + \frac{\sqrt{2}}{2}l_2 \cdot \frac{1}{2} - \eta_{hor,b} \cdot l_2\right)\right]}{a - l_1}; \qquad (41)$$

– from the right point (rig) to the left point (lef):

$$\frac{\varepsilon_{bu,k,rig,x}}{\varepsilon_{bu,k,lef,x}} = \frac{a - l_1}{a - (l_1 + l_2)}; \qquad (42)$$

$$\varepsilon_{bu,k,lef,x} = \frac{\varepsilon_{bu,k,rig,x} \cdot [a - (l_1 + l_2)]}{a - l_1}. \qquad (43)$$

Unknown deformations $\varepsilon_{s,k,rig,x}$ and $\varepsilon_{s,k,lef,x}$ we also determine from the proportionality conditions:

$$\varepsilon_{s,k,rig,x} = \frac{\varepsilon_{s,I} \cdot (a - l_1)}{a}; \qquad (44)$$

$$\varepsilon_{s,k,lef,x} = \frac{\varepsilon_{s,k,rig,x} \cdot [a - (l_1 + l_2)]}{a - l_1}. \qquad (45)$$

Then for the voltages, respectively, we can write

$$\sigma_{s,k,rig,x} = \varepsilon_{s,k,rig,x} \cdot E_s \cdot v_s(\lambda) \qquad \text{and}$$

$$\sigma_{s,k,lef,x} = \varepsilon_{s,k,lef,x} \cdot E_s \cdot v_s(\lambda).$$

Next, we determine the unknown parameter $x_{B,k}$ from the condition that the sum of the projections of all forces acting in the spatial section k on the x-axis is equal to zero: $\sum X = 0$, (see block II in Figure 2):

$$-\sigma_{s,k} \cdot m_d \cdot A_{s,d} + \sum R_{sc,up,i} \cdot \omega_{up} \cdot A_{sc,up,i} -$$
$$-\sum R_{s,i,rig} \cdot \omega_{rig} \cdot A_{s,i,rig} - \sum R_{s,i,lef} \cdot \omega_{lef} \cdot A_{s,i,lef} +$$
$$+\sum R_{sc,i,rig} \cdot \omega_{c,rig} \cdot A_{sc,i,rig} + \sum R_{sc,i,lef} \cdot \omega_{c,lef} \cdot A_{sc,i,lef} -$$
$$-\varphi_{10}\tau_{xy,u,Mt} \cdot A_{b,l_1} + \varphi_{10}\tau_{xy,u,Mt} \cdot A_{b,l_3} - \sigma_{b,1,rig} \cdot A_{b,*} -$$
$$-\sigma_{sc,1,rig} \cdot A_{sc,1,rig} - \sigma_{b,3,lef} \cdot A_{b,**} - \sigma_{sc,3,lef} \cdot A_{sc,3,lef} -$$
$$-X_{b,k} \cdot A_{b,k,x_B} - \varphi_{10}\tau_{xy,u,Mt} \cdot A_{b,l_1,ad} +$$
$$+\varphi_{10}\tau_{xy,u,Mt} \cdot A_{b,l_3,ad} - \sigma_{b,1,rig} \cdot A_{b,*,cir,ad} -$$
$$\sigma_{b,3,lef} \cdot A_{b,**,cir,ad} - X_{b,k} \cdot A_{b,k,core} = 0. \quad (46)$$

The following restrictions must be taken into account:

$$0.1h_0 \leq x_{B,k} \leq 0.3h_0; \qquad (47)$$

$$x_{B,k} \leq x_k; \qquad (48)$$

In equation (46), $X_{b,k}$ – the projection of the components of the stresses on the axis of x; A_{b,l_1} – is the area of concrete on the zone l_1; A_{b,l_3} – the area of concrete on the zone l_3; $A_{b,*,cir}$ – the area of concrete of the right sector

broken section (sector height $x_{B,1}$); $A_{b,**,cir}$ – the area of concrete left sector of the broken section (sector height $x_{B,3}$); $A_{b,l_1,ad}$ – the area of the concrete with a height Δx_1 of zone l_1; $A_{b,l_3,ad}$ – the area of the concrete with a height Δx_3 of zone l_3; $A_{b,*,cir,ad}$ – the area of the concrete part of the right sector altitude Δx_1; $A_{b,**,cir,ad}$ – square concrete of the left sector altitude Δx_3;

$$A_{b,k,core} = \Big((R - x_B)^2 \arccos\big((R - x_k)/R - x_B\big) -$$
$$-(R - x_k)\sqrt{2(R - x_B)(x_k - x_B) - (x_k - x_B)^2}\Big)\sqrt{2} \; -$$
the area of the core of the section of compressed concrete in the section k-k on the zone l_1;

$$A_{b,k,x_B} = \Big(R^2 \arccos\big((R - x_k)/R\big) -$$
$$-(R - x_k)\sqrt{2Rx_k - x_k^2}\Big)\sqrt{2} - A_{b,k,core} \; - \text{ the area}$$
of the arc of the upper fibres of circular cross-section; $\sum_{k=1}^{n_{rig}} R_{s,i,rig} \cdot \omega_{rig} \cdot A_{s,i,rig}$

$(\sum_{k=1}^{m_{rig}} R_{sw,i,rig} \cdot \omega_{rig} \cdot A_{sw,i,rig})$ – stress is stretched in the transverse reinforcement (cross clamps) to the right of the contour of the first segment of a parabola spatial $f_{par1,2,3}(x,y,z)$ (zone l_1);

$\sum_{k=1}^{m_{lef}} R_{sw,i,lef} \cdot \omega_{lef} \cdot A_{sw,i,lef}$ $(\sum_{k=1}^{n_{lef}} R_{s,i,lef} \cdot \omega_{lef} \cdot A_{s,i,lef})$ – stress is stretched in the longitudinal reinforcement (cross clamps) for the left loop of the second segment of a parabola spatial $f_{par1_r,2_r,3_r}(x,y,z)$ (zone l_3); h_0 – working height section.

$$A_{b,l_1} = \frac{\big(x_{B,k} + x_{B,1}\big) \cdot l_1}{2}; \qquad (49)$$

$$A_{b,l_3} = \frac{\big(x_{B,k} + x_{B,3}\big) \cdot l_3}{2}. \qquad (50)$$

The value $X_{b,k}$ for the midpoint (b$_k$) of the polyline section k (on the zone l_2) is:

$$X_{b,k} = \frac{\varphi_{z,1} \cdot \sigma_{bu,x,1} \cdot \varphi_{1,*} \cdot \left[a - \left(l_1 + \frac{\sqrt{2}}{2} l_2 \cdot \frac{1}{2} - \eta_{hor,b} \cdot l_2 \right) \right]}{a} +$$
$$+ \left(\pm \varphi_{10} \cdot \tau_{xy,u,Mt} \right) \cdot \varphi_{3,*}. \qquad (51)$$

Here $\varphi_{3,*}$ – is the transition coefficient from a cross-section to an oblique (oblique, – when the cross-section is located at an angle $\beta = 45°$, $\cos 45° = \frac{\sqrt{2}}{2}$); $\sigma_{b,ad,x,k}$ – normal stresses in the cross-section k are taken instead of stresses $\sigma_{bu,x,k}$, and tangential stresses $\tau_{xy,ad,Mt}$ are taken instead of stresses $\tau_{xy,u,Mt}$, these stresses are calculated by the formulas:

$$\sigma_{b,ad,x,k} = \sigma_{bu,x,k} - \sigma_{b,crc,x,k};$$
$$\tau_{xy,ad,Mt} = \tau_{xy,u,Mt} - \tau_{xy,crc,Mt}. \qquad (52)$$

The second supporting block of section k-k is separated from the reinforced concrete element by a spatial section formed by a spiral crack and a vertical section passing through the compressed zone of concrete through the end of the spatial crack front.

The balance of this block is ensured by fulfilling the following conditions.

The sum of the moments of all internal and external forces acting in the vertical longitudinal plane relative *to* the y-axis passing through the point of application of the resultant forces b_k in the compressed zone is zero $\sum M_{b,k}=0$ (see block II, Figure 2):

$$M_{bend,k} = \frac{\sigma_{s,k} + \sigma_{s,rig}}{2} \cdot (h_0 - 0.5 x_{B,k}) \cdot \frac{m_d}{2} \cdot A_{s,d} +$$
$$+ \frac{\sigma_{s,k} + \sigma_{s,lef}}{2} \cdot (h_0 - 0.5 x_{B,k}) \cdot \frac{m_d}{2} \cdot A_{s,d} +$$
$$+ \varphi_{7,*} \cdot R_s \cdot \eta_{hor,s} \cdot c_{i-1} \sum \omega_{*,cir} A_s - \varphi_{5,*} \cdot R_s \cdot \sum \omega_{*,cir} A_s +$$
$$+ \sum R_{s,i,rig} \cdot \omega_{rig,cir} \cdot A_{s,i,rig} \left[h_0 - 0.5 x_{B,k} - a_{s,i,rig} \right] +$$
$$\sum R_{s,i,lef} \cdot \omega_{lef,cir} \cdot A_{s,i,lef} \left[h_0 - 0.5 x_{B,k} - a_{s,i,lef} \right] +$$

$$+ \varphi_{7,*,rig} R_{s,rig} \sum \omega_{r,*,cir} A_{s,rig} \cdot \left(0.5 c_{inc,i-1} - 0.5 l_2 - z_{sw} \right) -$$
$$- \varphi_{5,*,rig} R_{s,rig} \cdot \sum \omega_{r,*,cir} A_{s,rig} -$$
$$- \varphi_{7,*,lef} R_s \sum \omega_{l,*,cir} A_{s,l} \cdot \left[l_3 (c_i) - 0.5 \cdot h \cdot \cos \alpha_0 +$$
$$+ 0.5 l_2 - z_{sw} \right] + \varphi_{5,*,lef} R_{s,lef} \cdot \sum \omega_{l,*,cir} A_{s,lef} +$$
$$+ q_{sw,rig} \cdot \frac{h}{2h+b} \cdot c \cdot \left(0.5 \cdot \frac{h}{2h+b} \cdot c \cdot -0.5 l_2 - z_{sw} \right) -$$
$$- q_{sw,lef} \cdot \frac{h}{2h+b} \cdot c \cdot \left[c - (l_1 + l_2) - 0.5 \cdot h \cdot \cos \alpha_0 + 0.5 l_2 - z_{sw} \right] +$$
$$+ \left(\varphi_9 \tau_{zy,u,Q} + \varphi_{11} \tau_{zy,u,Mt} \right) \cdot A_{b,l_1,ad} \cdot \left[\left(l_1 - \frac{l_1}{3} \cdot \frac{2 \cdot x_{B,k} + x_{B,1}}{x_{B,k} + x_{B,1}} \right) -$$
$$- (0.5 \cdot l_2 - \eta_{hor,b} \cdot l_2) \right] + \left(\varphi_9 \tau_{zy,u,Q} - \varphi_{11} \tau_{zy,u,Mt} \right) \cdot A_{b,l_3} \cdot$$
$$\cdot \left[\left(\frac{l_3}{3} \cdot \frac{2 \cdot x_{B,3} + x_{B,k}}{x_{B,3} + x_{B,k}} \right) + (0.5 \cdot l_2 + \eta_{hor,b} \cdot l_2) \right] +$$
$$+ \left(\varphi_{12} \cdot \tau_{zx,u,Q} + \varphi_{14} \cdot \tau_{zx,u,Mt} \right) \cdot A_{b,*,cir} \cdot \left[l_1 + (0.5 \cdot l_2 - \eta_{hor,b} \cdot l_2) \right] +$$
$$+ \left(\varphi_{12} \cdot \tau_{zx,u,Q} - \varphi_{14} \cdot \tau_{zx,u,Mt} \right) \cdot A_{b,**,cir} \cdot \left[l_3 + (0.5 \cdot l_2 + \eta_{hor,b} \cdot l_2) \right] +$$
$$+ \left(\varphi_9 \tau_{zy,u,Q} + \varphi_{11} \tau_{zy,u,Mt} \right) \cdot A_{b,l_1,ad} \cdot \left[\left(l_1 - \frac{l_1}{3} \cdot \frac{2 \cdot x_{B,k} + x_{B,1}}{x_{B,k} + x_{B,1}} \right) -$$
$$- (0.5 \cdot l_2 - \eta_{hor,b} \cdot l_2) \right] + \left(\varphi_9 \tau_{zy,u,Q} - \varphi_{11} \tau_{zy,u,Mt} \right) \cdot$$
$$\cdot A_{b,l_3,ad} \cdot \left[\left(\frac{l_3}{3} \cdot \frac{2 \cdot x_{B,3} + x_{B,k}}{x_{B,3} + x_{B,k}} \right) + (0.5 \cdot l_2 + \eta_{hor,b} \cdot l_2) \right] +$$
$$+ \left(\varphi_{12} \cdot \tau_{zx,u,Q} + \varphi_{14} \cdot \tau_{zx,u,Mt} \right) \cdot A_{b,*,cir,ad} \cdot \left[l_1 + (0.5 \cdot l_2 - \eta_{hor,b} \cdot l_2) \right] +$$
$$+ \left(\varphi_{12} \cdot \tau_{zx,u,Q} - \varphi_{14} \cdot \tau_{zx,u,Mt} \right) \cdot A_{b,**,cir,ad} \cdot \left[l_3 +$$
$$+ (0.5 \cdot l_2 + \eta_{hor,b} \cdot l_2) \right] + X_{b,k} \cdot A_{b,k,x_B} \cdot l_{b,i}. \qquad (53)$$

Here K_M, $K_{pr,M}$ – numerical coefficients, the same as in the formula (20); $a_{m,b}(c) = a - c - l_1 - \frac{1}{2} l_2$ – horizontal distance from the structural support to the center of gravity of the compressed concrete zone in section k; (a –distance from section I-I to the structural support). The projection c is assumed to be constant at each step of the iterative

process. Concise valves on either side of the cross-section in this equation is not taken into account in view of the smallness of the shoulder relative to the point b_k (because of the smallness of the parameter x_B); ϕ_5, $\phi_{5,r}$, $\phi_{5,1}$, $\phi_{7,r}$, ϕ_8 - parameters, taking into account the components of the "pin" effect in the armature (at each step of the iteration are taken as constants and are determined based on the model of the second level); ω_1, ω_2 – filling ratio plots shear stresses; $\eta_{hor,b}$ – the distance between the center b_k (the longitudinal axis of the beam) and the point b (see figure 2); $l_{b,i}$ – shoulder from the point b_k to the center of gravity of the cross-section with an area of $(x_k - x_{B,k}) \cdot \sqrt{l_2^2 + b^2}$ on the zone l_2.

Equation (53) determines the bending moment $M_{bend,k}$.

Next, we determine the transverse force from internal forces:

$$Q_k = R_{\sup,k,M} = \frac{M_{bend,k}}{a_{m,k}}. \qquad (54)$$

Here, $M_{bend,k}$ is found from the equation (53).

$$a_{m,k} = a_{m,b}(c) + K_M K_{pr,M}. \qquad (55)$$

The height of the compressed zone x_k in cross-section k-k between cross-sections I-I and III-III (see Figure 2) can be found from the ratio:

$$x_k = \frac{x_1 + x_3}{2}. \qquad (56)$$

x_1 – height of the compressed zone in section I-I for the equation (23); x_3 – height of the compressed zone in section III-III for the equation (24).

Enter the notation:

$$\eta_1 = \frac{x_{B,k}}{x_{B,k} + \Delta x_1}. \qquad (57)$$

Here, the height of the compressed zone $x_{B,k}$ for the k-k section is determined from equations (46), including and x_k. Then, for the increment of the height of the compressed zone in sections k-k and 1-1, we can write:

$$\Delta x_1 = x_k - x_1. \qquad (58)$$

On the other hand, if the relation (57) holds for sections 1-1, we can write $\eta_1 = \frac{x_{B,1}}{x_{B,1} + \Delta x_1}$. From here $x_{B,1}$ we get:

$$x_{B,1} = \frac{\eta_1 \cdot \Delta x_1}{\eta_1 - 1}. \qquad (59)$$

In this equation, the value Δx_1 is known. Similarly, by entering the notation η_3:

$$\eta_3 = \frac{x_{B,k}}{x_{B,k} - \Delta x_3}, \qquad (60)$$

Determine the height of the compressed zone in sections 3-3:

$$x_{B,3} = \frac{\eta_3 \cdot \Delta x_3}{(\eta_3 - 1)}. \qquad (61)$$

The sum of the projections of all forces acting in the spatial section **k** on the z-axis is zero ($\sum Z=0$, see block II, Figure 2):

$$q_{sw,rig} = \frac{tg\alpha}{h} \Big[q_{sw,lef} \cdot \eta_q \cdot \frac{h}{tg\alpha_0} -$$
$$-\varphi_{7,*} R_s \sum \omega_{*,cir} A_{s,*,cir} - \varphi_{7,*,rig} R_s \sum \omega_{rig,*,cir} A_{s,rig} +$$
$$+\varphi_{7,*,lef} R_s \sum \omega_{lef,*} A_{s,lef} - Q + R_{sup}$$
$$+\left(\varphi_{11}\tau_{zy,u,Mt} + \varphi_9 \tau_{zy,u,Q}\right) \cdot A_{b,l_1} +$$

$$+\left(\varphi_{11}\tau_{zy,u,Mt} - \varphi_9\tau_{zy,u,Q}\right)\cdot A_{b,l_3} +$$

$$\left(\varphi_{14}\cdot\tau_{zx,u,Mt} + \varphi_{12}\cdot\tau_{zx,u,Q}\right)\cdot A_{b,*,cir} +$$

$$\left(\varphi_{14}\cdot\tau_{zx,u,Mt} - \varphi_{12}\cdot\tau_{zx,u,Q}\right)\cdot A_{b,**,cir} +$$

$$Z_{b,k}\cdot A_{b,k,x_B} - \left(\varphi_{11}\tau_{zy,u,Mt} + \varphi_9\tau_{zy,u,Q}\right)\cdot A_{b,l_1,ad} +$$

$$\left(\varphi_{11}\tau_{zy,u,Mt} - \varphi_9\tau_{zy,u,Q}\right)\cdot A_{b,l_3,ad} +$$

$$\left(\varphi_{14}\cdot\tau_{zx,u,Mt} + \varphi_{12}\cdot\tau_{zx,u,Q}\right)\cdot A_{b,*,cir,ad} +$$

$$+\left(\varphi_{14}\cdot\tau_{zx,u,Mt} - \varphi_{12}\cdot\tau_{zx,u,Q}\right)\cdot A_{b,**,cir,ad} + Z_{b,k}\cdot A_{b,k,core}. \quad (62)$$

Here $Z_{b,k}$ – the projection of the components of stresses in the spatial section on the z-axis; $\varphi_{7,lef}$, $\varphi_{7,rig}$ – parameters that take into account the components of the "nagel" effect in the reinforcement (at each step they are taken as constants and determined based on the second – level model); Q – the transverse force in the section from the support to the k-k section.

For the midpoint (b_k) of a polyline spatial section k on the zone l_2 we can write:

$$Z_{b,k} = \left(\varphi_{12}\cdot\tau_{zx,u,Q} \pm \varphi_{14}\cdot\tau_{zx,u,Mt}\right)\cdot\frac{\sqrt{2}}{2} +$$

$$+\left(\varphi_9\cdot\tau_{zy,u,Q} \pm \varphi_{11}\cdot\tau_{zy,u,Mt}\right)\cdot\frac{\sqrt{2}}{2}. \quad (63)$$

Substituting in the formula (63) tangential stress $\tau_{zx,ad,Q}$ instead of $\tau_{zx,u,Q}$, $\tau_{zx,ad,Mt}$ instead of $\tau_{zx,u,Mt}$, $\tau_{zy,ad,Q}$ instead of $\tau_{zy,u,Q}$ and $\tau_{zy,ad,Mt}$ instead of $\tau_{zy,u,Mt}$ and using the dependencies $\tau_{zx,ad,Q} = \tau_{zx,u,Q} - \tau_{zx,crc,Q}$; $\tau_{zx,ad,Mt} = \tau_{zx,u,Mt} - \tau_{zx,crc,Mt}$; $\tau_{zy,ad,Q} = \tau_{zy,u,Q} - \tau_{zy,crc,Q}$; $\tau_{zy,ad,Mt} = \tau_{zy,u,Mt} - \tau_{zy,crc,Mt}$ the unknown $q_{sw,rig}$- the linear force in the clamps on the right side of the section is determined from equation (62).

The linear force in the clamps on the left side of the section ($q_{sw,lef}$) can be found from the relation:

$$q_{sw,lef} = q_{sw,rig} - \overline{\eta}_{11,*}\cdot\tau_Q; \quad (64)$$

Here $\overline{\eta}_{11,*} = \overline{\eta}_{11}\cdot b$ – is a coefficient that takes into account the projection lengths of inclined cracks on the left and right faces are approximately the same, i.e. $c_1 \approx c_2$, but $\pm\tau_Q$.

In this case, for the running force in the clamps, the condition must be met:

$$\frac{n\cdot R_{bt}\cdot A_{sw}}{u_s} \le q_{sw,lef} \le \frac{0.8\cdot R_{sw}\cdot A_{sw}}{u_s} - \overline{\eta}_{11}\cdot\tau_Q. \quad (65)$$

Here:

$$\sigma_{sw} = \frac{E_{sw}}{E_b}\cdot\sigma_{bt} = n\cdot R_{bt}; \quad \frac{n\cdot R_{bt}\cdot A_{sw}}{u_s} = q_{sw,lef,\min}; \quad (66)$$

$$\eta_{11}\cdot\tau_Q = \overline{\psi}_Q\cdot\tau_{pl,u} = \overline{\psi}_Q\cdot R_{ch}\left(\frac{c}{h_0}\right);$$

$$\eta_{11} = \frac{\overline{\psi}_Q\cdot R_{ch}\left(\dfrac{c}{h_0}\right)}{\tau_Q}. \quad (67)$$

The sum of the moments of internal and external forces in the transverse plane relative to the x-axis passing through the point of application of the resultant forces b_k in the compressed zone is zero ($\sum T_{b,k}=0$, see block *II,* Figure 2):

$$M_t = R_{\sup}\cdot\eta_{hor,b} + K_T\cdot\eta\cdot R_{\sup}\cdot a_m(c) =$$

$$= R_{\sup}\left(\eta_{hor,b} + K_T\cdot\eta\cdot a_m(c)\right) =$$

$$= -q_{sw,\sigma}\sqrt{l_2^2 + 4R^2}\cdot\left(h_0 - 0,5x_{B,k}\right) -$$

$$-q_{sw,rig}\cdot\frac{h}{tg\alpha}\cdot\left(0,5b - \eta_{hor,b}\cdot 2R\right) +$$

$$+q_{sw,lef}\,\eta_q\cdot\frac{h}{tg\alpha_0}\cdot\left(R + \eta_{hor,b}\cdot 2R\right) +$$

$$+\eta_{hor,b}\cdot b\cdot\varphi_{7,*}R_s\sum\omega_{*,cir}A_s -$$

$$-\left(h_0 - 0,5x_{B,k}\right)\cdot\varphi_{8,*}R_s\sum\omega_{*,cir}A_s +$$

$$-\left(0,5b + \eta_{hor,b}\cdot b\right)\cdot\varphi_{7,*,lef}R_s\cdot\sum\omega_{lef,*,cir}A_{s,lef} -$$

$$-\left(h_0 - x_{B,k} - a_{s,i,lef}\right)\cdot\varphi_{8,*,lef}R_s\sum\omega_{lef,*,cir}A_{s,lef} -$$

$$-\left(0,5b - \eta_{hor,b} \cdot b\right) \cdot \varphi_{7,*,\text{rig}} R_s \sum \omega_{rig,*,cir} A_{s,rig}$$

$$-\left(\text{h}_0 - x_{B,k} - a_{s,i,rig}\right) \cdot \varphi_{8,*,\text{rig}} R_s \sum \omega_{rig,cir} A_{s,rig} -$$

$$-R_{\text{sup}} \cdot \eta_{hor,b} + \left(\varphi_{11}\tau_{yz,u,Mt} + \varphi_9 \tau_{yz,u,Q}\right)$$

$$\cdot A_{b,l_1} \cdot \left[R - \eta_{hor,b} \cdot 2R - 2a'_{sc}\right] +$$

$$+\left(\pm\varphi_{11}\tau_{yz,u,Mt} + \varphi_9 \tau_{yz,u,Q}\right) \cdot A_{b,l_2} \cdot \left(R - 2a'_{sc}\right) +$$

$$+\left(\varphi_{11}\tau_{yz,u,Mt} - \varphi_9 \tau_{yz,u,Q}\right) \cdot A_{b,l_3} \cdot \left[R + \eta_{hor,b} \cdot 2R - 2a'_{sc}\right] +$$

$$+\left(\varphi_{14} \cdot \tau_{yx,u,Mt} + \varphi_{12} \cdot \tau_{yx,u,Q}\right) \cdot A_{b,*,cir} \cdot \left[R -\right.$$

$$\left.-\eta_{hor,b} \cdot 2R - a'_{sc}\right] + \left(\varphi_{14} \cdot \tau_{yx,u,Mt} -\right.$$

$$\left.-\varphi_{12} \cdot \tau_{yx,u,Q}\right) \cdot A_{b,**,cir} \cdot \left[R + \eta_{hor,b} \cdot 2R - a'_{sc}\right] +$$

$$+\left(\varphi_{11}\tau_{yz,u,Mt} + \varphi_9 \tau_{yz,u,Q}\right) \cdot A_{b,l_1,ad} \cdot \left[R -\right.$$

$$\left.-\eta_{hor,b} \cdot 2R - 2a'_{sc}\right] + \left(\pm\varphi_{11}\tau_{yz,u,Mt} +\right.$$

$$\left.+\varphi_9 \tau_{yz,u,Q}\right) \cdot A_{b,l_2,ad} \cdot \left(R - 2a'_{sc}\right) +$$

$$+\left(\varphi_{11}\tau_{yz,u,Mt} - \varphi_9 \tau_{yz,u,Q}\right) \cdot A_{b,l_3,ad} \cdot \left[R +\right.$$

$$\left.+\eta_{hor,b} \cdot 2R - 2a'_{sc}\right] + \left[\varphi_{14} \cdot \tau_{yx,u,Mt} +\right.$$

$$\left.+\varphi_{12} \cdot \tau_{yx,u,Q}\right] \cdot A_{b,*,cir,ad} \cdot \left[R - \eta_{hor,b} \cdot 2R - a'_{sc}\right] +$$

$$+\left(\varphi_{14} \cdot \tau_{yx,u,Mt} - \varphi_{12} \cdot \tau_{yx,u,Q}\right) \cdot A_{b,**,cir,ad} \cdot \left[R +\right.$$

$$\left.+\eta_{hor,b} \cdot 2R - a'_{sc}\right] + Y_{b,k} \cdot A_{b,k,core} \cdot h_i = 0 \ (68)$$

Here K_T ,– is a numerical coefficient that takes into account the peculiarity of the static loading scheme in terms of additional torques along the length of the structure; $K_{pr,T}$ – a coefficient that takes into account the relations between R_{sup} and T; $\phi_{7,\text{lef}}$, $\phi_{7,rig}$, $\phi_{8,\text{lef}}$, $\phi_{8,rig}$, – parameters that take into account the components of the "nagel" effect in the reinforcement. At each iteration step, these parameters are taken into account as constants and determined using the second-level model; $\eta_{hor,b,\text{lef}}$ – the distance between the center b_k (the longitudinal axis of the beam) and the point b_{lef} (see Figure 2, left part of the plot); α_0 – the angle of inclination of the middle section of the compressed concrete zone to the horizontal plane. The value of this

angle, based on experimental data, can be assumed to be 45^0 in the first approximation. The torque moment M_t can be expressed in terms of the bending moment using a relative parameter η taking into account the coefficient value K_T:

$$M_t = \eta \cdot M_{bend} .$$

The total torque moment M_t can be written as the sum of the torque moment expressed in terms of bending and the torque from the reaction of the support and the eccentricity of its application $\eta_{hor,b}$:

$$M_t = R_{\text{sup}} \cdot \eta_{hor,b} + K_T \cdot \eta \cdot R_{\text{sup}} \cdot a_m(c) =$$
$$= R_{\text{sup}} \left(\eta_{hor,b} + K_T \cdot \eta \cdot a_m(c)\right);$$

ω – filling ratio plot shear stresses in torsion in the compressed concrete in accounting for elastic-plastic work; $q_{sw,T}$ – linear stress to the clips that occur at the sides of the reinforced concrete element from the torque T (see figure 2); $q_{sw,\sigma}$ – linear stress to the clips that occurs on the bottom face of the concrete element from the torque T; h_i – shoulder from point b_k to the center of gravity of the cross-section area $(x_k - x_{B,k}) \cdot \sqrt{l_2^2 + b^2}$ at the zone l_2; $Y_{b,k}$ – projection components of the stresses in the broken section on the y-axis. For the midpoint (b_k) of the polyline section k on the section l_2, by analogy with (63), we can write:

$$Y_{b,k} = \varphi_9 \cdot \tau_{zy,u,Q} \cdot \frac{\sqrt{2}}{2} \pm \varphi_{13} \cdot \tau_{yx,u,Mt} \cdot \frac{\sqrt{2}}{2}. \ (69)$$

Substituting in (69) the tangent stress $\tau_{zy,ad,Q}$ instead of $\tau_{zy,u,Q}$, and $\tau_{yx,ad,Mt}$ instead of $\tau_{yx,u,Mt}$, and using the dependencies $\tau_{zy,ad,Q} = \tau_{zy,u,Q} - \tau_{zy,crc,Q}$;

$\tau_{yx,ad,Mt} = \tau_{yx,u,Mt} - \tau_{yx,crc,Mt}$ from the equation (68) the unknown M_t is found.

The sum of the projections of all forces acting in the spatial section **k** on the *y*-axis is zero ($\sum Y=0$, block *II*, see figure 2):

$$q_{sw,\sigma} = \frac{1}{\sqrt{l_2^2 + 4R^2}} \cdot \Big[-\varphi_{8,*,rig} R_s \sum \omega_{rig,cir} A_{s,rig} -$$

$$-\varphi_{8,*,lef} R_s \sum \omega_{lef,cir} A_{s,lef} - \varphi_{8,*} \cdot R_s \sum \omega_* A_s +$$

$$+\varphi_{13} \cdot \tau_{yx,u,Mt} \cdot A_{b,*} + \varphi_{13} \cdot \tau_{yx,u,Mt} \cdot A_{b,**} +$$

$$+Y_{b,k} \cdot x_{B,k} \cdot \sqrt{l_2^2 + b^2} + \varphi_{13} \cdot \tau_{yx,u,Mt} \cdot A_{b,*,ad} +$$

$$+\varphi_{13} \cdot \tau_{yx,u,Mt} \cdot A_{b,**,ad} + Y_{b,k} \cdot A_{b,k,x_B} + Y_{b,k} \cdot A_{b,k,core} \Big]. \quad (70)$$

Here ϕ_{8*} – is a parameter that takes into account the components of the "nagel" effect in the armature, which is taken as a constant at each iteration step and is determined using the second-level model [12,14,15].

From the equation (70) the unknown $q_{sw,\sigma}$ is found.

When composing a function of many variables, it is taken into account that $A_b = \phi(x)$, $a_{m,S} = \phi(c)$, $a_{m,b} = \phi(c)$, $a = const$, $c_\alpha = const$; $\sigma_{b,u} = const$; $\sigma_{b,I}$ is an unknown quantity, and the value $M_k = const$. The moment $M_I = f(c)$.

Transition coefficients ϕ_{10} etc. calculated iteratively, they are discrete constants at each step. The functions $f(x,y,z)$ of the diagonal large ellipse of the considered construction of a circular cross-section (with a smaller diagonal $b = R$ and a larger diagonal $a = l_1(c) + l_2 + l_3(c)$ can be written:

$$\frac{y^2}{(2l(c) + R\sqrt{2})^2} + \frac{z^2}{R^2} = 1. \quad (71)$$

Here $l_2 = R\sqrt{2}$; $a = l(c) + R\sqrt{2} + l(c) = 2l(c) + R\sqrt{2}$.

From this equation we get:

$$l(c) = \frac{-R\sqrt{2}}{2} + \sqrt{\frac{R^2}{2} + \frac{y^2 R^2}{4(R^2 - z^2)}}. \quad (72)$$

Then the projection of the spatial crack on the horizontal axis is determined from the expression:

$$c = l_1(c) + l_2 + l_3(c) = 2\sqrt{\frac{R^2}{2} + \frac{y^2 R^2}{4(R^2 - z^2)}} \le R \cdot 3\sqrt{2}. \quad (73)$$

Here $l_1(c) = l_3(c) = d\cos\alpha = d \cdot \cos 45° = d\frac{\sqrt{2}}{2}$;

$a = d\frac{\sqrt{2}}{2} + R\sqrt{2} + d\frac{\sqrt{2}}{2} = R \cdot 3\sqrt{2}$.

CONCLUSION

1. A calculated model and a beam calculated scheme are proposed for analyzing the complex limiting resistance of a reinforced concrete structure from the action of bending with torsion, taking into account the spatial nature of cracks in reinforced concrete elements of circular cross-section.

2. For the calculated forces, the resolving equations of equilibrium and the equations of deformations are compiled. In the considered calculated sections I–I and III–III, unknown components of the torque, height, and area of the compressed zone of concrete for an element of a circular cross-section are obtained. Similarly, using the equilibrium equations and strain equations for the spatial section k passing along the surface of the spatial crack, the components of the torque, the height of the compressed concrete zone, deformations and stresses in the reinforcement for the left and right parts of the section under consideration, and the load intensity in the clamps are obtained.

3. In the spatial section k, cut off by a spiral-shaped spatial crack, all the reinforcement intersected by this section is taken into account. The use of a complex broken section of a compressed concrete zone for practical calculations was due to the fact that cracking and destruction occurred in a certain volume according to linear dependencies at an angle close to the middle part of the broken section, where the maximum stress-strain state is reached.

4. In the area of the stretched zone of the spatial crack of a reinforced concrete round rod, the right and left contours of the longitudinal stretched working reinforcement and clamps are highlighted. The calculation scheme also takes into account the "nagel" effect in the stretched longitudinal and transverse reinforcement falling into this spatial section, the parameters of which are determined using a special model of the second level.

5. The static scheme of loading of a reinforced concrete element during bending with torsion was considered from the positions of the proportional ratio between the torques (the coefficient from the reaction of the support R_{sup}) along the length of the rod in the spatial section k and in the cross-sections (first and third).

REFERENCES

1. **Bondarenko V.M.** Computational models of the strength resistance of reinforced concrete. / V.M. Bondarenko, V.I. Kolchunov. – M .: ACB, 2004. – 472 p.

2. **Golyshev A. B.** Resistance of reinforced concrete / A. B. Golyshev, V. I. Kolchunov. – K .: Osnova, 2009 .- 432 p.

3. **Travush V.I., Karpenko N.I., Kolchunov Vl. I., Kaprielov S.S., Demyanov A.I., Bulkin S.A., Moskovtseva V.S.** Results of experimental studies of high-strength fiber reinforced concrete beams with round cross-sections under combined bending and torsion// Structural Mechanics of Engineering Constructions and Buildings 2020 –Vol.16 (4). pp. 290-297.

4. **Adheena Thomas, Afia S Hameed.** An Experimental Study On Combined Flexural And Torsional Behaviour Of RC Beams. *International Research Journal of Engineering and Technology.* 2017. Vol. 04. Issue 05. Pp. 1367–1370.

5. **Khaldoun Rahal.** Combined Torsion and Bending in Reinforced and Prestressed Concrete beams Using Simplified Method for Combined Stress-Resultants. *ACI Structural Journal.* 2007. Vol. 104. No. 4. pp. 402–411.

6. **Kolchunov Vl.I., Fedorov V.S.** Conceptual hierarchy of models in the theory of resistance of building structures // Industrial and civil engineering. 2020 –№8 – P. 16-23.

7. **C. Kim, S. Kim, K.-H. Kim, D. Shin, M. Haroon, J.-Y. Lee**. Torsional Behavior of Reinforced Concrete Beams with High-Strength Steel Bars. 2019. Structural Journal. Vol. 116, pp. 251–233.

8. **Kandekar, S.B., Talikoti, R.S.** Study of torsional behavior of reinforced concrete beams strengthened with aramid fiber strips. International Journal of Advanced Structural Engineering. 2018. Vol. 10, pp. 465–474. doi: 10.1007/s40091-018-0208-y.

9. **Křístek, V., Průša, J., Vítek, J.L.**: Torsion of Reinforced Concrete Structural Members. Solid State Phenom. 2018. Vol. 272, pp. 178–184.
doi:10.4028/www.scientific.net/SSP.272.178.

10. **Santhakumar R., Dhanaraj R., Chandrasekaran E.** Behaviour of retrofitted reinforced concrete beams under combined bending and torsion: A numerical study. Electronic Journal of Structural Engineering. 2007. No. 7. pp. 1–7.

11. **Ilker Kalkan, Saruhan Kartal.** Torsional Rigidities of Reinforced Concrete Beams Subjected to Elastic Lateral Torsional Buckling. International Journal of Civil and Environmental Engineering. 2017. Vol. 11. No.7. Pp. 969–972.

12. **Salnikov A., Kolchunov Vl., Yakovenko I.** The computational model of spatial formation of cracks in reinforced concrete constructions in torsion with bending (2015), Applied Mechanics and Materials Vols. 725-726 (2015) pp. 784–789.

13. **Iakovenko I., Kolchunov Vl.** (2017). The development of fracture mechanics hypotheses applicable to the calculation of reinforced concrete structures for the second group of limit states. Journal of Applied Engineering Science, Vol. 15(2017)3, article 455, pp. 366–375. (In English) doi:10.5937/jaes15-14662

14. **Demyanov A.I.** Development of a universal short two-console element to the resistance of reinforced concrete structures during torsion with bending / A.I. Demyanov Vl. I. Kolchunov, I. A. Yakovenko // Izvestiya VUZov. Textile industry technology. 2017. No. 4 (367). – pp. 258–263.

15 **Bernardo, L.** Modeling the Full Behavior of Reinforced Concrete Flanged Beams under Torsion. Applied Sciences. 2019. Vol. 9. doi:10.3390/app9132730.

16. **Pettersen J. S.** Non-Linear Finite Element Analyses of Reinforced Concrete with Large Scale Elements: Including a Case Study of a Structural Wall. Norwegian University of Science and Technology, 2014. 85 p.

17. **Nahvi H., Jabbari M.** Crack detection in beams using experimental modal data and finite element model. International Journal of Mechanical Sciences. 2005. Vol. 47. pp.1477–1497.

18. **Demyanov A., Kolchunov Vl.** The dynamic loading in longitudinal and transverse reinforcement at instant emergence of the spatial crack in reinforced concrete element under the action of a torsion with bending. Journal of Applied Engineering Science, vol. 15(2017)3, article 456, pp. 375–380. (In English) doi:10.5937/jaes15-14663

19. **Vishnu H. Jariwalaa, Paresh V. Patel, Sharadkumar P. Purohit.** Strengthening of RC Beams subjected to Combined Torsion and Bending with GFRP Composites. Procedia Engineering. 2013. Vol. 51. Pp. 282–289.

20. **Tsai H.-C., Liao M.-C.** Modeling Torsional Strength of Reinforced Concrete Beams using Genetic Programming Polynomials with Building Codes. 2019. KSCE Journal of Civil Engineering. Vol. 23, pp. 3464–3475 (2019). doi:/10.1007/s12205-019-1292-7.

21. **Arzamastsev S.A., Rodevich V.V.** To the calculation of reinforced concrete elements for bending with torsion. Izvestiya vysshikh uchebnykh zavod. Construction, 2015 –№9 - pp. 99-109.

22. **Karpyuk, V.M., Kostyuk, A.I., Semina, Y.A.** General Case of Nonlinear Deformation-Strength Model of Reinforced Concrete Structures. Strength Mater. 2018. Vol. 50, pp. 453–454. doi:10.1007/s11223-018-9990-9.

23. **Jan L. Vítek Jaroslav Průša, Vladimír Křístek, L.B.** Torsion of Rectangular Concrete Sections. ACI Symposium Publication. 2020. Vol. 344, pp. 111–130.

24 **Rahal, K.N.** Torsional strength of reinforced concrete beams. Canadian Journal of Civil Engineering. 2000. Vol. 27, pp. 445–453. doi:10.1139/cjce-27-3-445.

25. **Lin, W.** Experimental investigation on composite beams under combined negative bending and torsional moments. Advances in Structural Engineering. 2020. Vol. 24, pp. 1456–1465. doi:10.1177/1369433220981660.

СПИСОК ЛИТЕРАТУРЫ

1. **Бондаренко В.М.** Расчетные модели силового сопротивления железобетона. / В.М. Бондаренко, В.И. Колчунов. – М.: АСВ, 2004. – 472 с.

2. **Голышев А. Б.** Сопротивление железобетона / А. Б. Голышев, В. И. Колчунов. – К.: Основа, 2009. – 432 с.

3. **Травуш В.И., Карпенко Н.И, Колчунов Вл. И., Каприелов С.С., Демьянов А.И., Булкин С.А., Московцева В.С.** Результаты экспериментальных исследований сложно-напряженных балок круглого поперечного сечения из высокопрочного фиброжелезобетона // Строительная механика инженерных конструкций и сооружений. 2020 –т.16 – №4 – С. 290-297.

4. **Adheena Thomas, Afia S Hameed.** An Experimental Study On Combined Flexural And Torsional Behaviour Of RC Beams. *International Research Journal of Engineering and Technology*. 2017. Vol. 04. Issue 05. Pp. 1367–1370.

5. **Khaldoun Rahal.** Combined Torsion and Bending in Reinforced and Prestressed Concrete beams Using Simplified Method for Combined Stress-Resultants. *ACI Structural Journal*. 2007. Vol. 104. No. 4. pp. 402–411.

6. **Колчунов Вл.И., Федоров В.С.** Понятийная иерархия в теории сопротивления строительных конструкций // Промышленное и гражданское строительство. 2020 – №8 – с. 16-23.

7. **C. Kim, S. Kim, K.-H. Kim, D. Shin, M. Haroon, J.-Y. Lee**. Torsional Behavior of Reinforced Concrete Beams with High-Strength Steel Bars. 2019. Structural Journal. Vol. 116, pp. 251–233.

8. **Kandekar, S.B., Talikoti, R.S.** Study of torsional behavior of reinforced concrete beams strengthened with aramid fiber strips. International Journal of Advanced Structural Engineering. 2018. Vol. 10, pp. 465–474. doi: 10.1007/s40091-018-0208-y.

9. **Křístek, V., Průša, J., Vítek, J.L.**: Torsion of Reinforced Concrete Structural Members. Solid State Phenom. 2018. Vol. 272, pp. 178–184. doi:10.4028/www.scientific.net/SSP.272.178.

10. **Santhakumar R., Dhanaraj R., Chandrasekaran E.** Behaviour of retrofitted reinforced concrete beams under combined bending and torsion: A numerical study. Electronic Journal of Structural Engineering. 2007. No. 7. pp. 1–7.

11. **Ilker Kalkan, Saruhan Kartal.** Torsional Rigidities of Reinforced Concrete Beams Subjected to Elastic Lateral Torsional Buckling. International Journal of Civil and Environmental Engineering. 2017. Vol. 11. No.7. Pp. 969–972.

12. **Salnikov A., Kolchunov Vl., Yakovenko I.** The computational model of spatial formation of cracks in reinforced concrete constructions in torsion with bending (2015), Applied Mechanics and Materials Vols. 725-726 (2015) pp. 784–789.

13. **Iakovenko I., Kolchunov Vl.** (2017). The development of fracture mechanics hypotheses applicable to the calculation of reinforced concrete structures for the second group of limit states. Journal of Applied Engineering Science, Vol. 15(2017)3, article 455, pp. 366–375. (In English) doi:10.5937/jaes15-14662

14. **Демьянов А.И.** Разработка универсального короткого двух-консольного элемента к сопротивлению железобетонных конструкций при кручении с изгибом / А.И. Демьянов Вл. И. Колчунов, И. А. Яковенко // Известия ВУЗов. Технология текстильной промышленности. – 2017. №4(367). – С. 258–263.

15 **Bernardo, L.** Modeling the Full Behavior of Reinforced Concrete Flanged Beams under Torsion. Applied Sciences. 2019. Vol. 9. doi:10.3390/app9132730.

16. **Pettersen J. S.** Non-Linear Finite Element Analyses of Reinforced Concrete with Large Scale Elements : Including a Case Study of a Structural Wall. Norwegian University of Science and Technology, 2014. 85 p.

17. **Nahvi H., Jabbari M.** Crack detection in beams using experimental modal data and finite element model. International Journal of Mechanical Sciences. 2005. Vol. 47. pp.1477–1497.

18. **Demyanov A., Kolchunov Vl.** The dynamic loading in longitudinal and transverse reinforcement at instant emergence of the spatial crack in reinforced concrete element under the action of a torsion with bending. Journal of Applied Engineering Science, vol. 15(2017)3, article 456, pp. 375–380. (In English) doi:10.5937/jaes15-14663

19. **Vishnu H. Jariwalaa, Paresh V. Patel, Sharadkumar P. Purohit.** Strengthening of RC Beams subjected to Combined Torsion and Bending with GFRP Composites. Procedia Engineering. 2013. Vol. 51. Pp. 282–289.

20. **Tsai H.-C., Liao M.-C.** Modeling Torsional Strength of Reinforced Concrete Beams using Genetic Programming Polynomials with Building Codes. 2019. KSCE Journal of Civil Engineering. Vol. 23, pp. 3464–3475 (2019). doi:/10.1007/s12205-019-1292-7.

21. **Арзамасцев С.А., Родевич В.В.** К расчету железобетонных элементов на изгиб с кручением // Известия высших учебных заведений. Строительство, 2015 –№9 – с. 99-109.

22. **Karpyuk, V.M., Kostyuk, A.I., Semina, Y.A.** General Case of Nonlinear Deformation-Strength Model of Reinforced Concrete Structures. Strength Mater. 2018. Vol. 50, pp. 453–454. doi:10.1007/s11223-018-9990-9.

23. **Jan L. Vítek Jaroslav Průša, Vladimír Křístek, L.B.** Torsion of Rectangular Concrete Sections. ACI Symposium Publication. 2020. Vol. 344, pp. 111–130.

24 **Rahal, K.N.** Torsional strength of reinforced concrete beams. Canadian Journal of Civil Engineering. 2000. Vol. 27, pp. 445–453. doi:10.1139/cjce-27-3-445.

25. **Lin, W.** Experimental investigation on composite beams under combined negative bending and torsional moments. Advances in Structural Engineering. 2020. Vol. 24, pp. 1456–1465. doi:10.1177/1369433220981660.

Vladimir I. Kolchunov, Dr.Sc., Professor, Department of unique building and structures, South-Western State University, 94, 50 let Oktyabrya street, Kursk, 305040,Russia phone: +7 (910) 317-93-55; e-mail: vlik52@mail.ru

Bulkin S. Aleksandrovich, Chief Design Specialist of Urban planning institute of residential and public buildings (GORPROJECT), 105005, Russia, Moscow, Nizhny Susalny lane, 5, building 5A

Колчунов Владимир Иванович, доктор технических наук, профессор кафедры «Уникальные здания и сооружения», Юго-Западный государственный универсиет; 305040, Россия, г. Курск, ул. 50 лет Октября, дом 94; тел .: +7 (910) 317-93-55; e-mail: vlik52@mail.ru

Булкин Сергей Александрович, главный специалист-конструктор ЗАО «Городской проектный институт жилых и общественных зданий», Россия, 105005, Россия, г. Москва, Нижний Сусальный пер., 5, стр. 5А